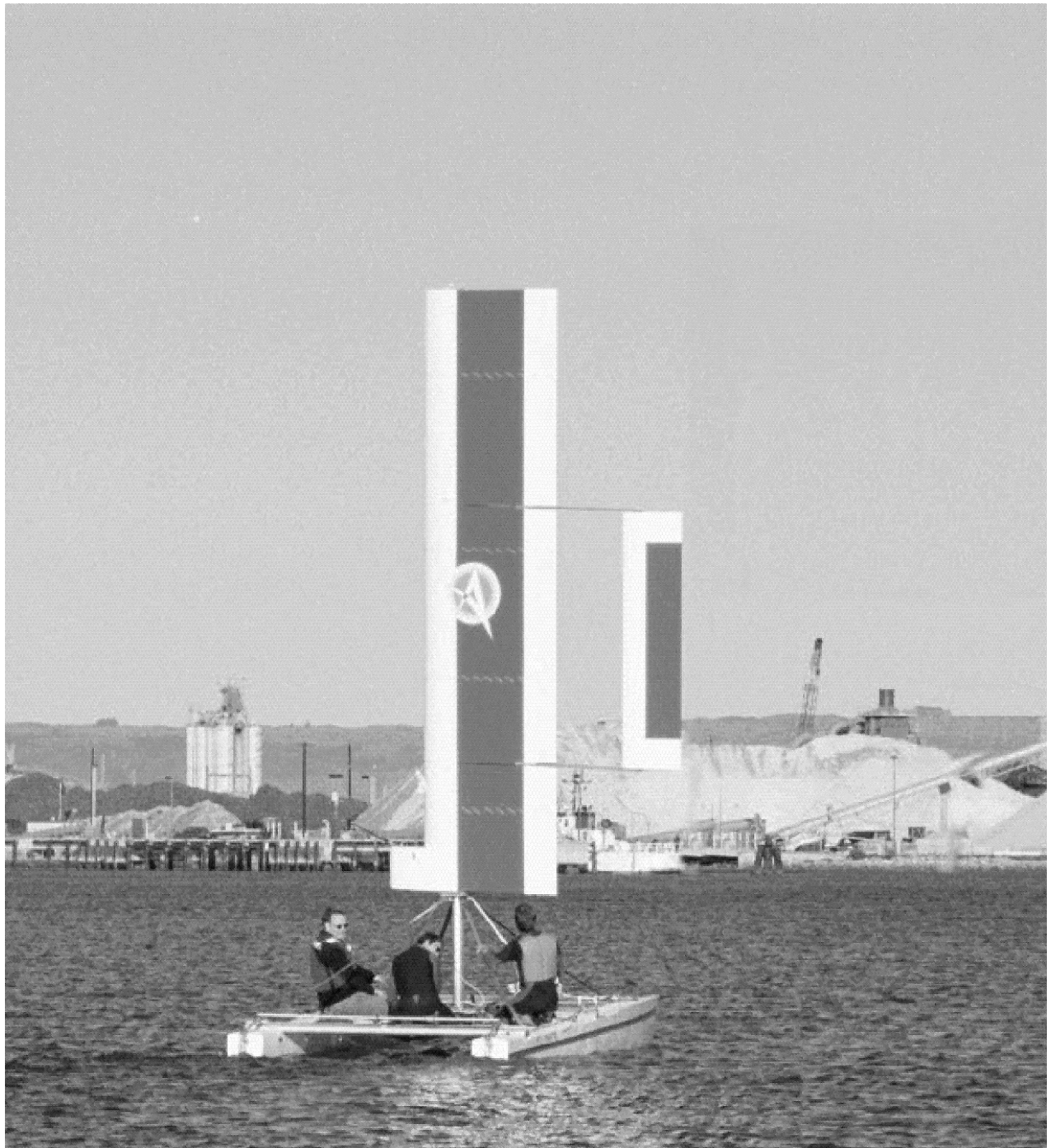


Catalyst

Journal of the Amateur Yacht Research Society

Number 16

April 2004



An Autonomous Wing-Sailed Catamaran

Gabriel H. Elkaim
Ph.D. Thesis



Is it a boat, a plane, something in between?

This presentation details the Atlantis project, whose aim is the design, development, and experimental testing of an autonomous wind-propelled marine craft. Functionally, such a vehicle is the marine equivalent of an unmanned aerial vehicle (UAV), and would serve similar purposes. The Atlantis project has been able to demonstrate an advance in control precision of a wind-propelled marine vehicle from typical commercial autopilot accuracy of 100 meters to an accuracy of better than one meter with a prototype based on a modified Prindle-19 light catamaran. The project involves substantial innovations in three areas: windpropulsion system, overall system architecture, and sensors.

The wind-propulsion system is a rigid mass-balanced wing-sail mounted vertically on bearings which allow free rotation in azimuth about a stub-mast. Aerodynamic torque about the stub-mast is trimmed using a flying tail mounted on booms aft of the wing. This arrangement allows the wing-sail to automatically attain the optimum angle to the wind, and weathervane into gusts without inducing large heeling moments.

[This article is an extract from Gabriel Elkaim's PhD thesis which was submitted as an entry for the John Hogg Prize. The thesis, for which Dr Elkaim was awarded his PhD by Stanford University, centred upon the autonomous control of the craft, however we have extracted for Catalyst readers only those (less-mathematical) parts dealing with the design and (next edition) the construction of the wingsail.

Please note that the equations and figures are numbered as in the original document. - Editor]

The sensor system uses differential GPS (DGPS) augmented by a low-cost attitude system based on accelerometer- and magnetometer-triads for position and velocity measurements.

Experimental tests were performed, requiring the catamaran to sail on a precise track through the water, in the presence of currents, wind, and waves. Using the identified system models, a high-performance estimator/controller was implemented and tested on the full-scale prototype. These controllers were indeed quite successful, tracking the line to within 0.3 meters.

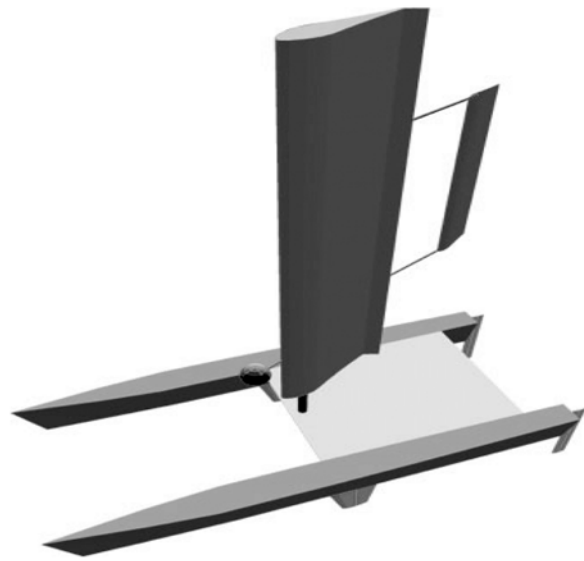
The Wingsail

The concept of using a wing upon a sailboat has been around almost as long as aircraft themselves. Many previous designers have come to the false conclusion that adequate lift coefficient could only be achieved with an asymmetric (cambered) wing. This led them to designs that tack by flipping up over the top of the mast, often leaving the wing inclined at 45 degrees (the flip does not rotate the wing a full 180 degrees). The disadvantage of this arrangement is that the weight associated with the flipping mechanism is usually large enough to negate any increased propulsive efficiency by virtue of increase hull drag. Also, with the inclined wing designs only the vertical projection of the wing acts to propel the boat. This again results in a loss of propulsive efficiency.

Design Choices

The most visibly unique aspect of the Atlantis project is the wingsail propulsion system, as shown in Figure 5-1. The design considerations and goals are: equivalent performance to the original sail system, low actuation force, and the ability to precisely control the resulting system.

A sloop rig sail can achieve a maximum lift coefficient of 0.8 if the jib and sail are perfectly trimmed. Realistically, an operating maximum lift coefficient is 0.6. The design goal of the Atlantis wing is to achieve a maximum lift coefficient of 1.8. Since this allows the wing to generate three times the force of an equivalently sized sail, the wing area is reduced to one third of the area of the original sails. Because the drag characteristics of the wing are much improved, the performance of the wingsailed catamaran should be superior to the original configuration. At worst, the wing will yield equivalent performance.



Fundamental to the goal of autonomous operation is the requirement that the actuation of the sail be simple. In the case of a conventional sail, this would be extremely expensive in terms of actuator cost and power requirements as the forces required are quite large. Additionally, the complex nature of the aerodynamics of a sail makes any sort of precise control of the sail difficult to accomplish. In order to achieve precision control of the catamaran, the disturbances generated by the propulsion system must be minimized. Fundamentally, this requirement forces the design away from a conventional sail.

Figure 5-2 shows the design evolution of the wingsail for the Atlantis. The design choices are on the right of the figure. The choices are designated by the triangles, with the losing choice to the left, and the winning choice to the right. The text explains the problem with the losing choice.

The steps of the evolution are each detailed in later sections. The design evolution begins with a choice between a conventional cloth sail or a rigid wingsail. Then the choice is between a symmetrical or asymmetrical section. Following the symmetry choice, one must choose between an existing section and a custom designed airfoil section. With the section design complete, the next issue is to trim the wing aerodynamically or mechanically. Lastly, four possible configurations for the wing and trimming surface are considered. The series of choices lead the design to a self-trimming wingsail with a conventional tail, using a custom designed airfoil section for the appropriate Reynolds number. The remainder of this chapter considers each choice in detail.

(Opposite) Figure 5-1 The engineering model of the Atlantis. The wing sail is 5.37 meters tall and has a chord of 1.45 meters. The self-trimming tail is used to balance the aerodynamic moments. The model includes a spherical mass attached to the leading edge of the wing to bring the mass center of the wing/tail combination in line with the stub-mast. In the actual prototype, the ball mass was replaced with an electronics pod attached to the forward end of the lower wing section.

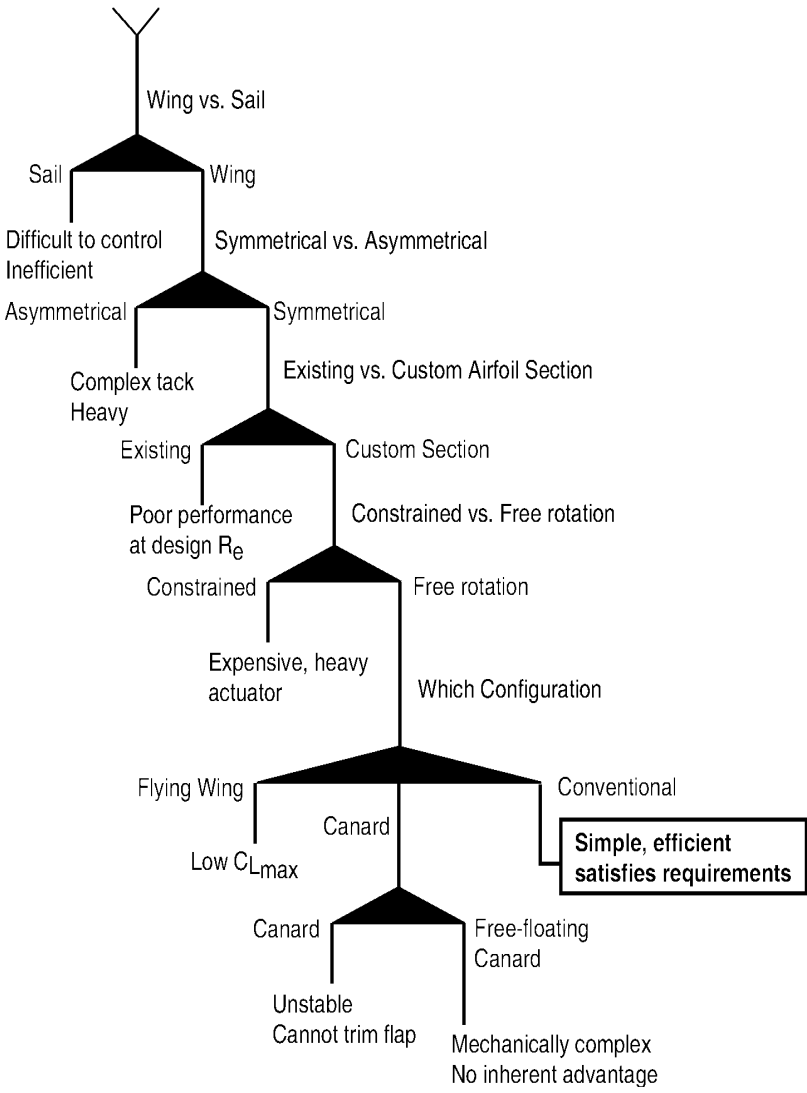


Figure 5-2 The design evolution of the propulsion system. The design choices are on the right of the figure in black. The choices are designated by the triangles, with the winning choice to the right. The text explains the problem with the losing choice. The series of choices lead the design to a self-trimming wingsail with a conventional tail, using a custom designed airfoil section for the appropriate Reynolds number.

Wingsail Description

The chosen wingsail is 5.37 meters tall and has a chord of 1.45 meters. It is constructed in three sections: the lower section which includes the forward electronics/ballast pod, the middle section to which the tail is attached by twin booms, and the upper section. The wingsail is built entirely of marine grade plywood covered in polyester fabric and is suspended by a spherical roller bearing at the top of the stub-mast. It is stabilized by a needle roller bearing around the stub-mast at the bottom of the wing. This allows the wing to rotate freely through 360 degrees without significant resistance. An engineering diagram of the wing is shown in Figure 5-3.

Wing Versus Sail

There are three main reasons to use a wing instead of a sail: efficiency, less actuation force required, and self-trimming. The first and most obvious is that a rigid wing is far more efficient than a cloth sail. Though some attention needs to be given to Reynolds number effects, the coefficient of lift, C_L , has a maximum of 1.8 for the Atlantis wingsail versus typically 0.8 for a perfectly trimmed sloop rig (jib and mainsail). Also, the Lift/Drag (L/D) ratio of the Atlantis wingsail is in the 10 - 30 range, whereas the L/D of the conventional sail is in the 3 - 5 range. Further, a cloth sail suffers from aeroelastic collapse when pointed high into the wind (the sail is said to be luffing). This causes a great deal of drag when sailing closehauled and effectively limits how high the boat can point into the wind. The rigid wing, by contrast, suffers no aeroelastic problems; it can point straight into the wind with very little drag, no flapping, no whipping about, and no noise, while effectively reefing the wing. In fact, the feathered wing-tail combination has much less drag than the bare mast. This is demonstrated in Figure 5-4, which shows two sections (cylinder and airfoil) that have the same net drag (including both viscous and pressure forces). Because the two sections have the same drag, the ability to reef a sail (or reduce the area of the sail) is moot when using a rigid wing because the wing has far less aerodynamic load on it than the bare mast itself.

The second main reason to use a wingsail for propulsion is less force is required to actuate the wing itself. A cloth sail is fixed to the mast, and trimmed from the boom. Since the center of pressure of the sail is aft of the leading edge, the trim force must overcome a portion of the lift of the

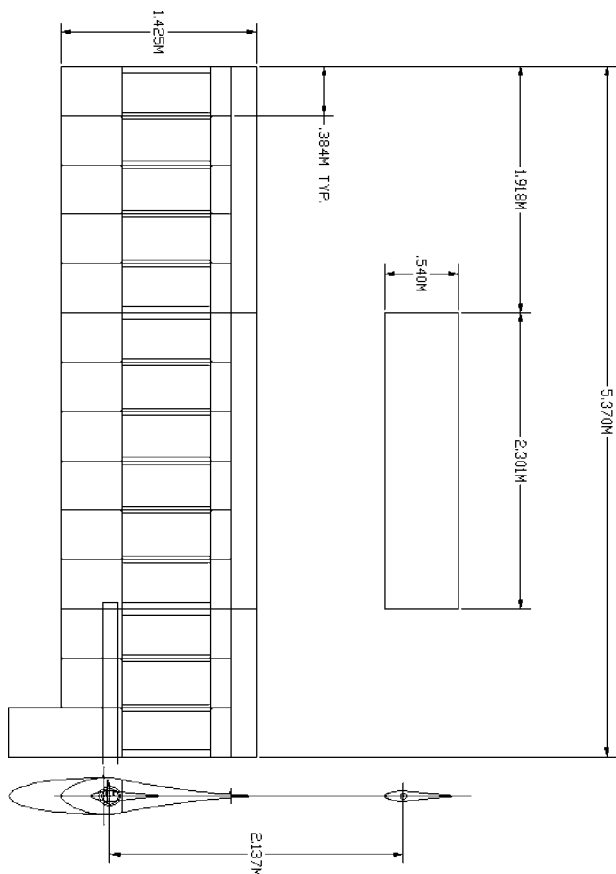


Figure 5-3 An engineering layout of the wingsail. This drawing shows the dimensions of the wing, the three sections, and the rib layout pattern. On the bottom it shows the overhead view, including the electronics pod at the front of the wingsail. (Details of the wing structure and construction will be published in the next part.)

sail. Inspection of a conventional sailboat shows a large block and tackle with eight or more loops of line attached to the boom is required to trim the main sail. With a winch, an additional 8:1 mechanical advantage is required to hold the boom in. To control this effectively in an automatic manner, a very large and fast-acting actuator is required. These types of actuators quickly become very expensive and a typical one would cost more than the entire budget for the project. By contrast, the wing can be designed to pivot near the center of pressure of the wing itself. The wingsail is turned to an angle of attack either directly or through an auxiliary trimming surface. In either case, this is accomplished with a small DC motor and can be actuated quickly and inexpensively. The cost effectiveness of this design is the main reason it was used for this project.

The third main advantage of the wingsail over the conventional sail is the ability to make the wingsail self-trimming. The benefit of this is that the wing will absorb gusts without transmitting the force of the gusts through to the guidance system. By decoupling the propulsion system from the guidance system through passive stability (self-trimming), the control system design is greatly simplified. Through proper arrangement of the flying surfaces, the wingsail will readjust automatically to a change in either wind speed or wind direction, with no intervention from pilot or control system.

The self-trimming capability makes the wingsail ideal for an autonomous sailboat because it eliminates the requirement for a very large and fast acting actuator to constantly retrim the sails. The only time that direct intervention into the trim control of the wing is required is when the wing crosses the longitudinal centerline of the boat, or when guarding against excessive heeling moments. During this maneuver, the flap and tail are reversed from their previous positions. Note that in a conventional sense this corresponds to tacking (when the wind is from the bow of the boat) and jibing (when the wind is from the stern of the boat). The maneuvers using the wingsail are both very gentle and controlled because the bearings allow the sail to rotate 360 degrees about the mast without interference, and the wing can point straight into the wind without ill effects.

Conventional sails have one serious advantage: due to their sharp leading edge, they tend to be insensitive to Reynolds number variation. This alone may explain why they have persisted on modern designs even after the preponderance of evidence has demonstrated that wings are vastly superior. The other advantage that cloth sails may have over rigid wings is weight: for sails below a certain size, a rigid wing will almost certainly be heavier. This is due to the square-cubed law with respect to the strength of structures.

Above a mast height of approximately 20 meters, the structure of the mast could just as easily be incorporated into the spar of a wing. In [93], a race between two similar catamarans with a rigid wing and a conventional sail was analyzed. The winged catamaran had superior aerodynamic thrust on all points of sail, but the difference of ~150 pounds required a wind speed of greater than 8 knots for the superior aerodynamics to result in superior boat speed. The greater weight led to greater drag on the hulls due to the extra displacement of water. In the race, all legs that were raced at wind speeds greater than 8 knots were won by the winged catamaran, but all legs below 8 knots were won by the conventionally sailed catamaran.

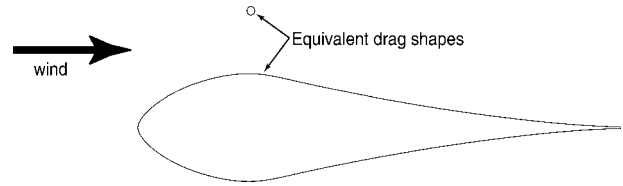


Figure 5-4 Demonstration of the equivalent drag sections at Reynolds number of 229,000. The small solid cylinder and the airfoil section have the same total drag (including both skin friction and pressure drag terms). A rigid wing need not be capable of reefing (or reducing its total area) in order to protect the boat. As demonstrated above, the wing (if allowed to pivot freely) will have much less force on it than the bare mast itself.

Reynolds Number Effects

As mentioned previously, the Reynolds number effects of the wingsail section design must be accounted for in order to maximize the efficiency of the wing. Ignoring these Reynolds number effects has been the largest failing of wingsails to date, resulting in sections with poor performance in the field, and, in turn, delaying the transition to rigid wings on sailboats.

The Reynolds number, Re , is defined as:

$$Re = \frac{\rho V L}{\mu} \quad (\text{EQ 5.1})$$

where ρ is the density of the medium, V is the velocity of the flow, L is the characteristic length, and μ is the viscosity of the medium. The Reynolds number represents the ratio of kinematic or inertial forces to the viscous forces in the fluid (that is, the ratio of force required to push the fluid out of the way versus the force required to slip through the “gooeyness”).

Typically, insect flight has Re on the order of 100s to 1000s, bird flight and models in the 100,000s, small aircraft in the millions range, and large aircraft in the tens of millions range. The Reynolds number characterizes the flow’s ability to negotiate the curves of a section without separation. Illustrative of this is Figure 5-5 which is reproduced from [123] and demonstrates the different drag characteristics of a 2-D cylinder as a function of Reynolds number.

In the case of airfoil sections, several effects come into play at low Reynolds numbers that make design of high lift sections difficult. Most of these are discussed at length in [122]. Flow about an airfoil at low Reynolds numbers is almost entirely laminar.

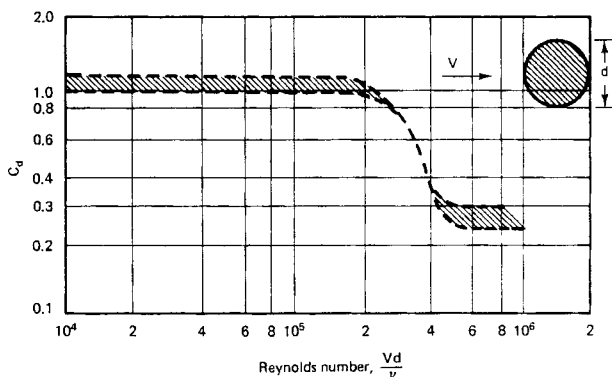


Figure 5-5 Effect of Reynolds number on the drag coefficient of a 2-D cylinder. At low Reynolds numbers, the drag remains constant. This is consistent with separation occurring just aft of the maximum diameter of the cylinder. As the Reynolds number increases, the now turbulent flow is able to negotiate the curvature better. This causes the drag coefficient to drop until the point that the flow remains attached approximately 1/3 of the way down the back side of the cylinder, at which point the drag coefficient once again becomes constant with increasing Reynolds number.

Thus the flow can withstand neither sharp radii nor severe adverse pressure gradients without separation (and consequential very large drag rise). In the case of airfoil sections, the flow separates, but then reattaches causing a laminar separation bubble whose flow eddy results in a very large increase in the base drag of the section. Furthermore, as soon as the angle of attack of the section is increased, the laminar separation bubble bursts, causing large scale flow separation and effectively limiting the maximum lift coefficient, C_L , attainable.

In [25], the designers demonstrate a knowledge of the difficulties in designing good sections at these Reynolds numbers, but fail to capitalize on this knowledge and find an appropriate design. They correctly identify the proper Reynolds number range for sail operation as 200,000 to 1.2 million, and complain that “good low Reynolds number aerodynamic data applicable to sails is not readily available.” Unfortunately, low Reynolds number computer codes had not yet reached maturity at the time they were investigating superior sails. Thus, while correctly identifying the problem, they did not find an appropriate solution.

The reason that low Reynolds number airfoil sections do not exist for this range has to do with the unique requirements of sailing vehicles. Typically, this Reynolds number range corresponds to small model airplanes, usually gliders. The differences are

subtle and will be exposed in detail forthwith.

First, both the model glider and the sailboat require a high lift/drag (L/D) ratio. In a glider, this corresponds to glide distance. In a sailboat, this corresponds to the ability to point upwind. Second, both a model glider and a sailboat require a high maximum C_L . In the case of the glider, this corresponds to slow flight while circling tightly in thermals, or a minimum sink condition; in a sailboat, the configuration is maximum speed while sailing across or down wind.

At this point, the requirements are essentially the same and there should be a large body of work on appropriate sections that can be used for the sailboat wing. Given the constraints of designing a low Reynolds number airfoil section for the wingsail, there are a few details to consider. Firstly, the wingsail section must be suitable for the Atlantis to sail on both port and starboard tacks.

Symmetry

An airfoil section can be made either symmetrical or asymmetrical. An asymmetrical section can always achieve a higher maximum lift coefficient and a higher lift/drag ratio than a symmetric section. Symmetric sections have the advantage of identical lift characteristics with both positive and negative angles of attack. Symmetry arguments become important in sailing vessels because a sailboat is required to sail equally well on both port and starboard tacks and thus the section must be symmetrical. The model glider is rarely required to fly inverted, and certainly not for long periods of time. Thus model glider sections are always asymmetrical in order to maximize the L/D . Certain sailboats, including the designs in [118], [26], and [34], attempt to capture the maximum L/D by using an asymmetrical section, but then tack and jibe “over-the-top.” This means that the wing is pinned midway up its span, then flipped to a horizontal position, and finally the bottom and top ends are then switched as the tack or jibe is completed. This is demonstrated in Figure 5-6. Needless to say, this results in an extremely heavy structure at the pin joint as well as an exposed support or mast which greatly increases the overall drag on the superstructure of the boat. It also makes wing control during this maneuver difficult in strong winds.

Using modern airfoil design techniques and a simple plain flap, one can achieve very close to the maximum C_L of an asymmetrical section. Thus, the increased weight, complexity, drag, and loss of the

Image © Boatek (Gen. Quinton)

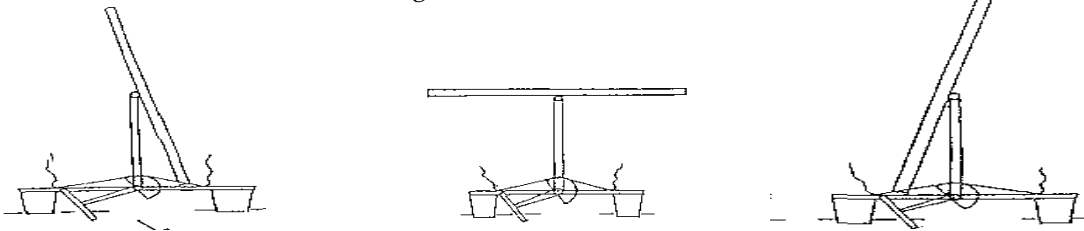


Figure 5-6 Frames from video showing the Boatek wingsail performing an over-the-top tack. From left to right, the boat is first turned into the wind. As the angle to the wind approaches zero, the wing (in this case, wings) are pivoted horizontally midway up the wing. As the boat turns through the wind, the wings are lowered to the opposite position from the first frame and secured. The top and bottom ends of the wings having been swapped, the tack is now complete

ability to self-trim in an asymmetrical design seem hardly worth the effort. Indeed, the ease of handling a symmetric section which does not pivot horizontally about the mast allows an increase in wing area, thus making up for the lower maximum lift coefficient. Although some continue to advocate over-the-top designs, they seem to stem more from novelty than an true understanding of aerodynamic trade-offs.

Airfoil Section Design

The first step in designing the best performing airfoil section is determining the appropriate Reynolds number, then achieving the best lift with the most benign characteristics.

It is desirable for the section to achieve a maximum lift coefficient of 1.8 at a Reynolds number range of 200,000 to 250,000. This can be aided by a simple plain flap of constant flap/chord ratio. The pitching moment coefficient must be small with the flap in trail so as to be easily balanced by the tail. Then, the greater the lift/drag ratio, the better will be the upwind performance of the Atlantis. In order to match the total force on the original sail at a wind speed of 5 knots with a theoretical lift coefficient of 1.8, Equation 5.1 is solved for a resulting Reynolds number of 229,000. Figure 5-7 shows the wind velocity required to achieve this Reynolds number as a function of angle from the true wind. This is based on the assumption that the sailboat can sail at one third of the true wind speed. The figure shows that the range of minimum wind speeds is from 3.8 to 6 knots.

The wing has one third the area of the sails, but generates three times the lift at its design point. This was chosen to enable a comparison of performance between the wing and sail. Note that the final design gets better as the Reynolds number increases. The difficult thing to achieve is performance at low

Reynolds numbers. Once that has been achieved, the same airfoil section can achieve a higher coefficient of lift at greater Reynolds number. In order to achieve the desired goals of maximum lift coefficient of 1.8, lift/drag ratio of better than 20, and optimization for a Reynolds number of 229,000, a rather unusual design emerges. First, in order to achieve the high lift coefficients at low Reynolds numbers, a very thick section is required, where the entire lift is generated on the forward section, typical of the Liebeck “rooftop” sections. The boundary layer requires a trip-strip that will force the transition from laminar to turbulent, placed symmetrically on the top and bottom surfaces. Typically, these trip-strips are a thick material with a zig-zag leading edge that is affixed to the surface at the desired location. The zig-zag causes a small-scale vortex to form which pulls in the higher energy flow outside of the boundary layer, and though viscous drag increases, separation (and thus form drag) is delayed.

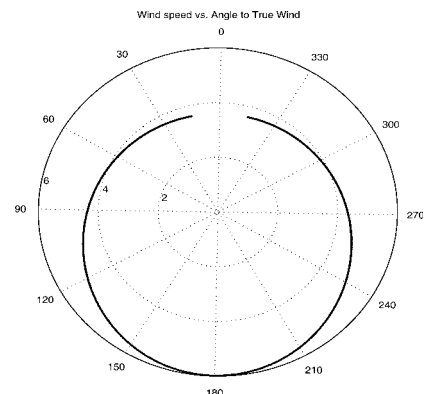


Figure 5-7 Polar plot of the true windspeed versus the angle to the true wind. This plot shows the velocity of the wind to reach a minimum speed necessary to have a Reynolds number of at least 229000. The sailboat is assumed to be able to sail at one third the speed of the true wind. This results in a range of 3.8 knots at 15 degrees to the true wind to 6 knots running directly before the wind.

In addition to the short, flat pressure distribution on the section, the entire aft portion of the section is given to pressure recovery of the flow preventing flow separation from the section surface. Thus the back three quarters of the section do not contribute at all to the lift, but merely ensure that the airflow can recover to free stream conditions gracefully.

Analysis Tools

In order to design the wing and tail sections, modern computational fluid dynamics (CFD) computer codes are used to predict performance and refine the design of the sections. The two main codes utilized for this are Ilan Kroo's PANDA and Mark Drela's XFOIL.

PANDA, which is an acronym from **P**rogram for **A**nalysis and **D**esign of **A**irfoils, was developed by Professor Ilan Kroo in the 1980's at Stanford University[84]. The program computes and graphically displays the pressure distribution (in coefficient form) on airfoil sections in subsonic flow. For a particular airfoil with coordinates stored in a standard text file, the program calculates the inviscid pressure distribution over the airfoil at a specified angle of attack and Mach number; lift and pitching moment about the $\frac{1}{4}$ -chord point are also computed. The analysis is done with remarkable speed (less than a second) so that the effects of changes in angle of attack or airfoil geometry can be studied easily.

The program also computes the boundary layer properties based on this inviscid pressure distribution. The location of transition, laminar or turbulent separation, and total drag are computed based on integral boundary layer methods. It is possible to specify a position for "transition grit" or "trip-strip" on the upper and lower surfaces to force transition or model surface roughness.

A major feature of the PANDA program is its provision for rapidly changing the airfoil geometry. This is done by positioning the cursor over the part of the airfoil to be changed and clicking the mouse button. A smoothly-faired bump (with specified but editable height and width) is added to the section at this point and the new pressure distribution is quickly redrawn (the normalized pressure is referred to as the coefficient of pressure, C_p). In this way the airfoil can be rapidly reshaped to produce a desirable C_p distribution.

XFOIL is a computational fluid dynamics (CFD) code that was written by Mark Drela in 1986 at the Massachusetts Institute of Technology (MIT), see [39], [40], and [41]. The main goal was to combine the speed and accuracy of high-order panel methods with the fully-coupled viscous/inviscid interaction

method used in the more sophisticated codes developed by Drela and Giles. A fully interactive interface was employed from the beginning to make it much easier to use than the traditional batch-type CFD codes. Several inverse modes and a geometry manipulator were also incorporated early in XFOIL's development, making it a fairly general airfoil development system.

XFOIL is a much more full-fledged code than PANDA, able to operate well into the low Reynolds number regimes with excellent predictive capabilities. It also includes the ability to use either free or forced boundary layer transitions and to predict lift and drag polars to just beyond the maximum lift coefficient.

Wing Section

Section development starts with a National Advisory Committee for Aeronautics (NACA, the predecessor of the present NASA) 00xx section to probe the design space. The NACA section is then modified using PANDA until reasonable performance was achieved. At this point, the section coordinates are transferred to XFOIL which is used to iterate on the pressure distribution and boundary layer trip-strip location until the desired results are achieved.

The first attempt used a NACA 0015 airfoil section. Originally developed in the 1930's, the NACA 0015 is a symmetrical section with a thickness to chord ratio of 15%, and designed as a turbulent section. While this airfoil section is known to have poor performance at low Reynolds numbers, as the *de facto* standard for symmetrical sections, it functions as a benchmark against which to compare all other attempts. Further, land yacht designers are using NACA 00xx sections almost exclusively in their successful designs.

Part of their rationale behind this choice is the observation that the main drag source is not parasitic drag but rather induced drag. Since induced drag is largely a function of the aspect ratio of the wing and the load carried by the wing, the effect of airfoil section is minimal. This gross analysis, however, fails to take into consideration the loading variation of the wing and the problems of stall and separation. While the wing might be flying at a coefficient of lift below stall, sections of it might be above due to variations in wind speed with height (wind gradient) or effective twist due to the same effect. These problems can only be addressed with high maximum lift coefficient and the NACA 0015 simply cannot provide it. Figure 5-8 shows the poor performance of the NACA 0015 at low Reynolds numbers, where the flow is largely laminar. Note the laminar

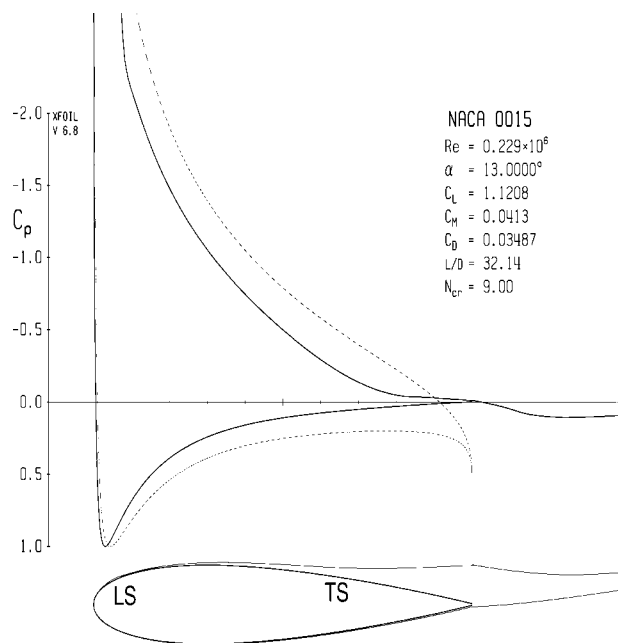


Figure 5-8 XFOIL results for NACA 0015 airfoil at Reynolds number of 229,000 and C_L of 1.12. This is a turbulent boundary layer section. Note the very sharp pressure spike corresponding to the leading edge of the airfoil (with a $C_p < -4.0$ for a lift coefficient of 1.12) that will most likely cause separation. Indeed the laminar separation bubble is marked by “LS” and the trailing edge turbulent separation indicative of stall is marked “TS.”.



Figure 5-9 Close up view of the laminar separation bubble on NACA 0015 airfoil at Reynolds number of 229,000.

At this scale, the enlargement and then, farther along, contraction of the boundary layer is clearly visible. Inside the enlarged section an eddy vortex is stationary and consumes energy in its rotation. This results in increased drag. As the angle of attack increases, the vortex tightens and eventually bursts, resulting in turbulent boundary separation and stall

separation bubble (“LS”) on the top surface, the turbulent separation (“TS”) indicating a stall, and the rather low lift/drag ratio at this condition.

The laminar separation bubble, indicated by the “LS” in Figure 5-8, can be seen more clearly if we zoom into the section. In Figure 5-9, we take a closer look at the laminar separation bubble and can clearly see the effect of the boundary layer growth and subsequent contraction as the flow reattaches following the laminar separation. While the presence of the laminar separation bubble is invisible from a macroscopic view, it nonetheless affects the entire flow of the section. The maximum lift coefficient attainable is directly related to the presence or absence of the laminar separation bubble and the manner in which the section stalls is also driven by its presence. When a laminar separation bubble is present, the stall is likely to occur at the point of the bubble rather than at the trailing edge. This results in a sudden loss of lift and increase in drag, rather than a gradual loss of lift and increase in drag.

The final design, after many iterations, results in a rather unusual shape. First, the final wing section is enormously thick, with a thickness to chord ratio of over 21%. The distribution of that thickness is predominately toward the nose of the section. This is consistent with the requirement that most of the lift is generated at the front part of the section, in front of the boundary layer trip-strip, while the entire aft section is there only for pressure recovery.

Close inspection of the section will show that the post boundary trip curvature is in fact concave, making construction using a normal cloth covering somewhat of a challenge. As the cloth covering shrinks, it will tend to pull off of the curved rear section of the airfoil since a straight line connecting the point of maximum cross section and the end just before the flap hinge is shorter than the actual surface. Looking at the pressure distribution in Figure 5-10, one can immediately see the design challenges that were presented and how they were solved. Note the absence of either laminar separation bubbles or turbulent separation at the end of the section. This is at a C_L of 1.04, with no flaps deployed.

Again, it is important to point out the salient features of the pressure distribution shown in Figure 5-10. Observe the flat top of the pressure distribution, corresponding to a uniform suction on the upper front surface. The pressure begins its recovery just after the trip strip located at the 22% chord point and very smoothly recovers back to free stream pressure without separation. Note that the flow is actually accelerating on the lower surface

below the stagnation point. This causes the upward slope of the lower line in the pressure distribution, indicating some suction existing at the maximum chord point of the final wing section. Also, just after the trip-strip lies a very smooth pressure recovery all the way to the rear point of the airfoil section. Reemphasizing, there are no laminar separation bubbles and no turbulent separation. This airfoil section is not close to stall but will stall gently from the rear progressing forward, resulting in a very gradual loss of lift and increase in drag. This is important due to the varying nature of the wind. When the wind is highly variable, a conventional section like the 0015 will often abruptly stall and lose lift.

Tail Section

The design methodology for the tail section is virtually identical to that of the main wing section. The differences here are that the tail section will not be flapped, and because of its narrower chord, the design Reynolds number is much lower, around 44,000. Again, the same methods are employed, first using PANDA and then converging on the final design with XFOIL. A trip-strip is needed and has been placed at the 20% chord-wise location due to the inability to withstand adverse pressure gradients. Figure 5-11 demonstrates the flat forward rooftop pressure distribution along with the gradual recovery to free stream pressures. Further investigation demonstrates that the tail has an expected lift coefficient of 0.75 before turbulent separation begins at the rear of the section. This once again allows a gradual and smooth change in the lift and drag characteristics of the section without compromising the maximum lift that can be generated. Note that there are no laminar separation bubbles, and at the lift coefficient of 0.5, there is no trace of turbulent separation at the rear of the section. Thus, all of the design requirements of the tail section are met and the relatively large thickness to chord ratio allows a robust structure to be built using conventional materials such as foam, plywood, and polyester fabric.

Flap/Chord Ratio

In order to increase the coefficient of lift of the main wing section and obviate the need for “over-the-top” tacking and jibing, a simple plain flap is used to increase the camber of the wing. Figure 5-13 shows the pressure distribution with the flap deployed at 45 degrees. Note that the flow separates off the back of the flap causing an increase in drag. Unfortunately, at these low Reynolds numbers, the flow cannot negotiate the curvature of the flap hinge

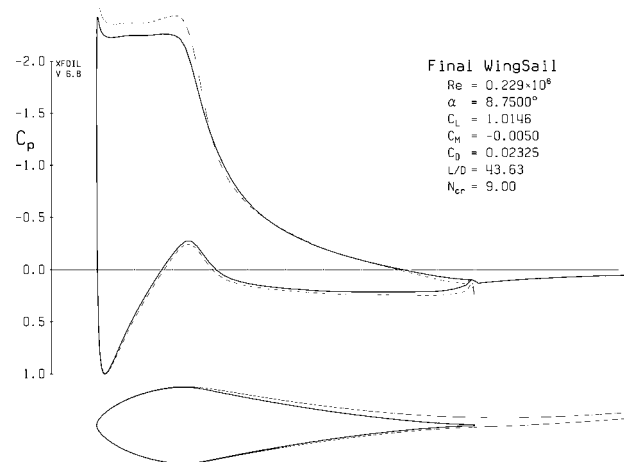


Figure 5-10 Final wing sail airfoil section and pressure distribution, Reynolds number of 229,000 and a coefficient of lift of 1.0. The pressure distribution is shown in the standard manner, with $-C_p$ along the y-axis, and the normalized chord along the x-axis. This section demonstrates a “rooftop” pressure distribution that rises immediately to a value of -2.5 and stays there for the 25% of the airfoil section. There, the boundary layer is tripped to force a transition to a turbulent section, and a long slow pressure recovery is used to prevent separation.

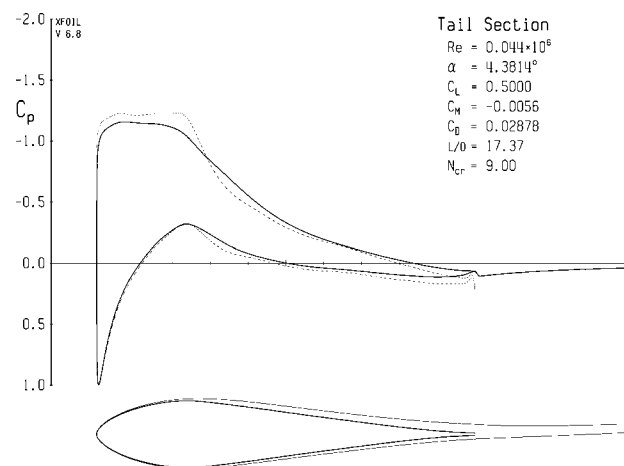


Figure 5-11 Pressure distribution of the final tail section at a Reynolds number of 44,000 and a lift coefficient of 0.5. This section is very similar to the final wing section. It shows the same “rooftop” flat forward section on the pressure distribution. The lift coefficient is 0.5, with no trace of laminar separation bubbles nor any turbulent separation. Further analysis using XFOIL indicates that this section can reach a C_L of 0.75 before stall.

regardless of where it is placed on the airfoil section. This means that the flow on the low pressure side of the flap will separate as soon as it is deflected more than a degree or so. With this constraint, the issue becomes one of trading the separated flow and subsequent drag for increased effective camber of the section and increased lift. Thus, the low Reynolds number pushes the design toward a very small flap/chord ratio and large deflection. In other words, a small trailing edge tab deflected a great deal will turn the flow enough to give effective camber, while giving the flow only the smallest area from which to separate.

In order to find the optimum flap/chord ratio, a grid point search is performed using XFOIL in order to find the minimum drag at a coefficient of lift of 1.8. The flap/chord ratio is varied from 1% to 40% in 1% increments and the optimum is found to be at 13%. Figure 5-12 shows the results of these computations. Both the maximum attainable lift coefficient as well as the lift to drag ratio at that lift coefficient are presented. It can be seen that both reach their maxima close to a 13% flap to chord ratio.

The final shape for the main wing section is presented in Figure 5-13, with the flap deflected 45 degrees. The aggregate plots of the lift to drag coefficients for the final section with the flap deployed can be found in Figure 5-14. The plot shows that there exists an “efficient boundary” where the lift/drag ratio is maximized for a given lift distribution.

This will then become the basis of control: once the desired lift coefficient is determined, the correct flap setting can be chosen to minimize the drag. Note that above a C_L of 1.8, the drag continues to increase without any further increase in lift. This is expected from the increase in separation of the flow, and as predicted is gradual. Looking at the data in a different way, it is useful to visualize the lift/drag ratio as a function of either lift, drag, or angle of attack. Note that the angles of attack involved are uniformly small, implying that the control over the tail must be precise or the tail, and subsequently the wing sail, will be stalled for the duration of the sail test. The lift/drag ratios are plotted against the above-mentioned parameters in Figure 5-15. It can be seen to have a peak at an angle of attack of 2-3 degrees, with the flap set at 25 degrees.

This, then, is the most efficient configuration at which to sail upwind. All other points of sail require that the wing sail provide the maximum force and then be modulated downwards as the threat of capsize increases.

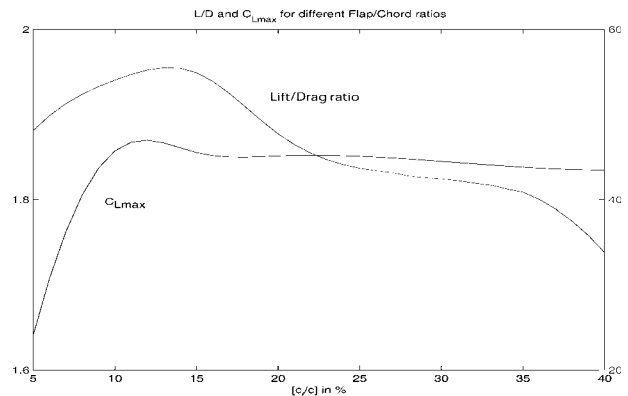


Figure 5-12 Results of the grid point search for optimum flap performance. Maximum attainable lift coefficient is plotted in blue and the lift to drag ratio is plotted in green. Note that while they both have a maximum in between 10% and 15% flap to chord ratios, the lift/drag maximum is much sharper in the area of 13%.

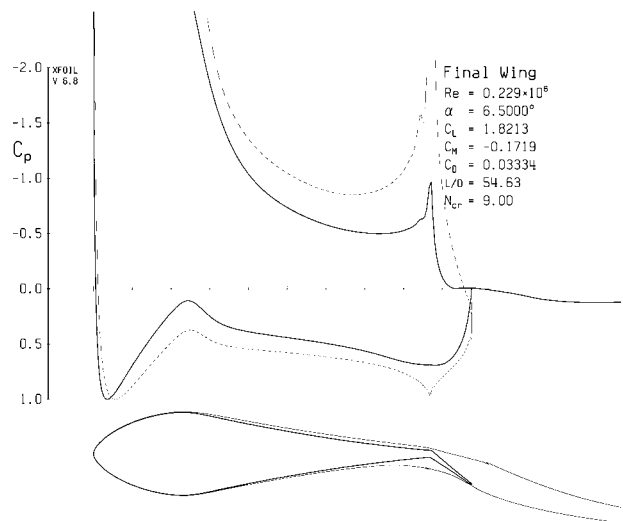


Figure 5-13 Pressure distribution of main wing sail section with flap deployed, Reynolds number of 229,000 and a coefficient of lift of 1.8. In order to preserve the lift/drag ratio of the section with the flap deployed, while attaining a high C_{Lmax} , a small trailing edge flap is used. At this Reynolds number, any flap deflection will result in separation.

Thus, a narrow chord flap is deflected a large amount to generate a high effective camber. At the same time, this design minimizes the area of separation, and hence drag.

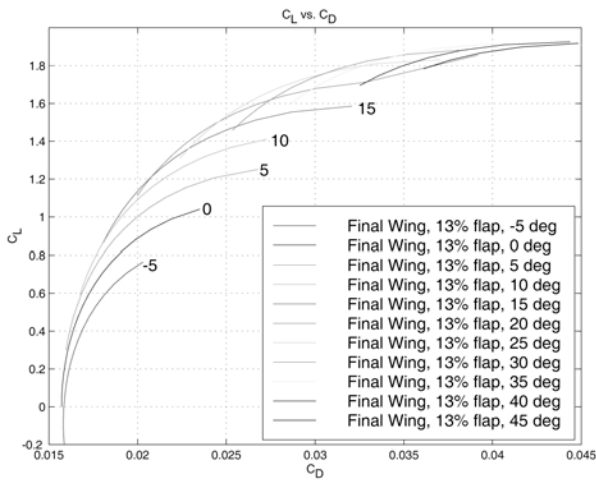


Figure 5-14 Coefficients of lift vs. drag for the final wing section with flap deployed at a Reynolds number of 229,000. For a given C_L , there is a unique flap angle that yields the minimum drag for that lift coefficient forming an efficient boundary. This will later be used to control the wing; once the desired lift is set, the flap is tuned for minimum drag based on that lift coefficient.

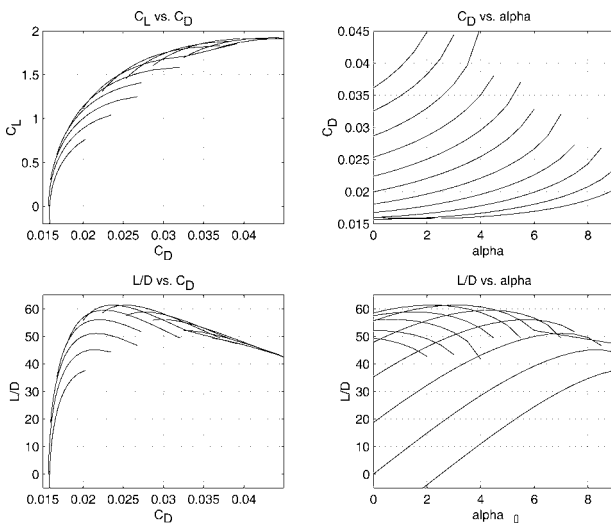


Figure 5-15 Aerodynamic polars for the main wing sail with flap deployed at a Reynolds number of 229,000. The lift/drag ratio peaks at around 62 with a corresponding angle of attack of 2 degrees. This corresponds to a lift coefficient of approximately 1.3 and a flap deflection of 20 degrees. Note that at this flap deflection, the lift/drag ratio remains high over the range of 0 to 4 degrees angle of attack

Wing/Tail Configuration Analysis

Two possibilities exist for actuating the wing and controlling its angle of attack.

The first possibility is to control the angle of attack mechanically using an actuator that rotates the wing about the mast. This has the advantage of quick actuation, and correct placement of the rotation axis can keep the forces low. However, the variability of the wind will require high frequency actuation to keep the wing correctly trimmed. Furthermore, the entire range of angles of attack between zero lift and stall is less than 10 degrees. This translates into the actuator requirement to track the wind very closely indeed. The other possibility for angle of attack control is to use an auxiliary surface to trim the wing aerodynamically. The auxiliary surface can take the form of a tail behind the wing (conventional), a tail in front of the wing (canard), or attached to the trailing edge of the wing (flying wing). The actuator requirement in this case is to move the trimming surface only. By designing the auxiliary surface in such a way as to have the wing/surface assembly be passively stable with respect to angle of attack, the entire system will track the relative wind automatically. This is a great advantage over active control in terms of actuation effort, simplicity of design, and overall performance.

With the main wing section and tail section designed, the various arrangements of wing and tail needed for the Atlantis to sail can now be considered. The first requirement for wing and tail consideration is stability with respect to change in wind direction or velocity. Based on the design of the wing section and the conclusions reached above, the configuration must be able to hold a C_L of 1.8 with a flap deflection of 45 degrees. This is important because the deflected flap will cause an increase in the pitching moment of the wing section about the mast. Formally, these requirements can be written as:

$$C_m = 0 \tag{EQ 5.2}$$

The pitching moment of the entire wing/tail system about the mast should be zero. That is, the system is in trim, and:

$$\frac{d}{d\alpha}(C_m) < 0 \tag{EQ 5.3}$$

The change in pitching moment with a change in angle of attack should be negative. The wing/tail system should be stable with respect to angle of attack.

The other considerations are mechanical complexity, control power, and a minimum swept

radius of the farthest point away from the mast. The minimum swept radius constraint is due to the fact that in order to remove the coupling between angle of attack of the wing sail and heeling angles, the wing/tail assembly must be mass balanced about the mast so that pitch and roll angles do not induce changes in angle of attack. A tail heavy wing/tail assembly would result in an increase in angle of attack with roll angle, thus inducing instability in close hauled conditions.

Fekete et al. in [48] perform a simplified analysis of the conventional and canard configurations. In this section, that analysis is refined by using higher fidelity models for downwash and induced drag as well as correcting for aspect ratio effects. Furthermore, two other configurations, the “flying wing” and the “free-floating canard,” are analyzed using the same tools.

Conventional Layout

The conventional layout is what would occur if a normal airplane were sliced in half down the longitudinal axis, turned on its side, and affixed to the mast through the quarter chord point of the wing. The arrangement, pictured in Figure 5-16 has the wing forward, followed by a tail some distance back. This has the immediate disadvantage of being tail heavy. This requires ballast forward to place the center of mass at the quarter chord point of the main wing. In terms of a wing, ballast is useless weight. Because the weight must be attached to the wing, it raises the center of gravity of the boat. This makes the design more prone to capsizing. Additionally, the swept radius of the tail is quite far back. This means that in close quarters (such as berthing), the tail may swing out beyond the catamaran hulls and strike an adjacent ship.

A top down view of Figure 5-16 is presented in Figure 5-17 and shows all of the force and moment vectors acting on the wing sail and tail. Note that in order to balance or trim the wing sail, the moment about the pivot point must be zero. To guarantee passive gust stability, the derivative of the moment equation with respect to the angle of attack must be negative. This implies that a perturbation of the angle of attack in a positive sense will cause a negative (or nose down) pitching moment which will reduce the angle of attack, and likewise a negative angle of attack perturbation will cause an increase in the pitching moment (nose up) and will increase the angle of attack. Also note that the reference to up and down is simply a convention to relate the wing terminology back into the intuitive reference of flight. In fact, there is no up or down, rather port or

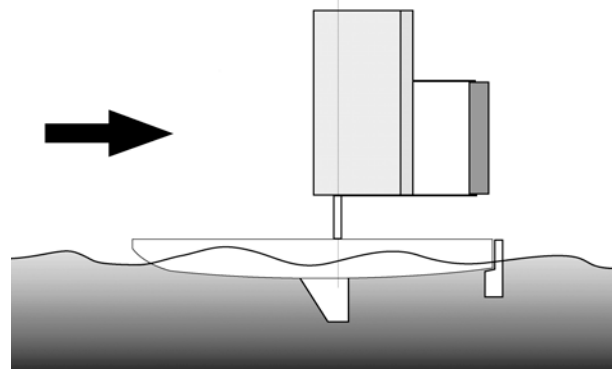


Figure 5-16 Conventional configuration for the wing sail and tail arrangement. This is the equivalent of a conventional airplane sliced in half down the length of the airplane, turned sideways and mounted on the stub-mast. This configuration has the inherent disadvantage that the wing design is tail heavy. This requires ballast to bring the mass center of the wing/tail assembly in line with the stub-mast. Additionally, this configuration has the farthest point of the wing/tail far away from the stub-mast. Thus, it sweeps out a large radius, making it impossible to use external stays on the stub-mast above the wing.

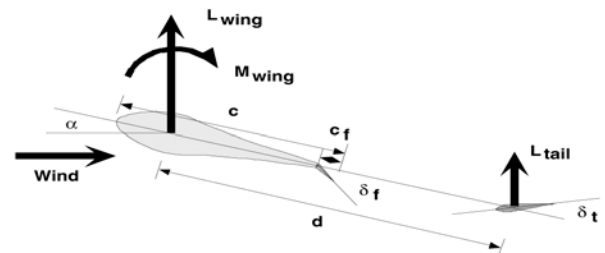


Figure 5-17 Force vectors on the conventional configuration. The forces and moments on the conventional configuration are displayed along with the relevant angles and distances. The wing is “flying” at an angle of attack, α , which in turn generates lift and pitching moment associated mostly with the trailing edge flap. This pitching moment must be resisted by the lift force on the tail.

starboard, and that the important feature which is missing from these equations which would be present if this were in fact an aircraft are the gravity terms. They do not, however, come into play in this stability analysis.

Canard

An alternate configuration is the “canard,” where the tail is placed in front of the wing as pictured in Figure 5-18. The immediate advantage professed for this arrangement is that both the main wing and the tail are lifting in the same direction and therefore must be more efficient. In an aircraft, this turns out to be untrue. A canard aircraft has trim and stall problems that must be dealt with and can usually be designed for either passive stability, or efficiency (i.e., reduced induced drag), but never both.

The overwhelming advantage a canard has for the sailboat propulsion system is that it is more easily balanced about its neutral point, making the entire setup lighter. Also, depending on the distances that occur for trim and stability, it is possible that the radius swept by the canard arrangement can be made small. If the swept radius is small enough to fit within the existing guy wires of the original mast, then the canard can be fit around the existing mast like a sleeve. This would negate the need for a free-standing stub-mast making the structure of the mast much easier to design. Figure 5-19 shows the vectors and key distances on the canard configuration. Once again, it is required that the moment balance be zero (trim) and that the change in moment be negative (stability).

The problem occurs with the robustness of this approach. The solution to the equations exists for only one value of flap deflection. For instance, if the trim and stability criteria are solved for a flap deflection of 45 degrees and a coefficient of 1.8, then when the flap is deflected less than 45 degrees, the canard configuration is not stable, and will attempt to swap ends. Furthermore, if the trim and stability criteria are solved for zero flap deflection, then at a high lift coefficient the canard will not be able to hold the main wing at a sufficient angle of attack. The canard itself will not be able to generate sufficient lift to balance the nose-down pitching moment induced by the large lift on the main wing.

Unfortunately, the canard configuration must be chosen to be stable, or to have a high maximum lift coefficient, but it cannot do both! Thus the canard configuration is not acceptable for this project. If the additional complexity of a flap on the canard is included, then it would be possible to adjust the flap on the canard in such a way as to compensate for the additional moment generated by the deflected flap on the main wing.

This is exactly the same problem that canard aircraft have. Very few of them have flaps on the main wing for decreased landing speeds. In fact, those few that do have flaps on their main wings

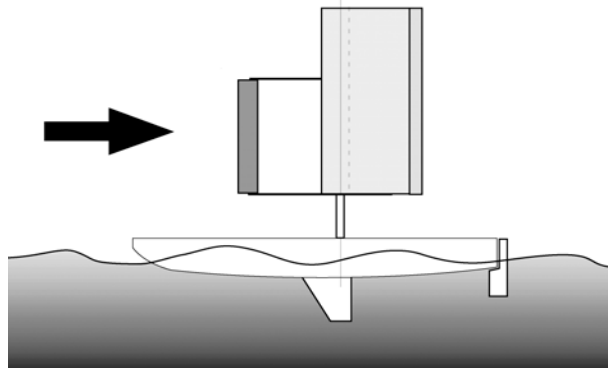


Figure 5-18 Canard configuration of the main wing sail and tail. The canard configuration has the trim surface (or tail) in front of the main wing. The advantage of this is that it can be made to have its mass center coincide with the stub-mast. Also, there exists the possibility that the swept radius can be made such that it is possible to have the entire canard/wing assembly fit inside guy wires that stabilize the mast.

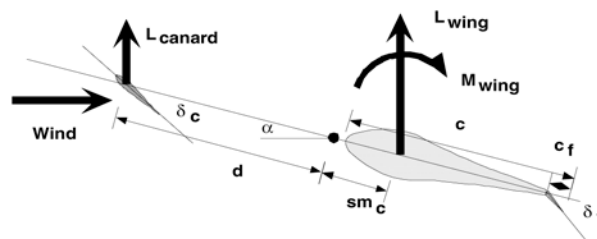


Figure 5-19 Force vectors on the canard configuration. The canard configuration has the purported advantage of efficiency, due to the fact that both the main wing and canard lift in the same direction. It truth, canard configurations can be made to be efficient (low induced drag) or passively stable, but never both. As a wingsail, the canard offers the advantage of already having its mass center near the pivot point. This minimized the ballast required and results in a lighter overall rig.

look to some rather exotic solutions, such as having a variable sweep canard that changes the longitudinal center of the canard as the flaps are deployed. For an excellent treatment of the subtleties of canard designs, see [85] and [98].

Flying Wing

If the desire were to minimize the swept radius of the wing, then certainly the flying wing would represent the optimal approach. Flying wings, however, almost always rely on washout of the tips to provide stability. That is, the tips of the rearward swept wings are twisted nose down and act somewhat like a conventional tail. To make a symmetrical flying wing sail requires both trim and stability without any wing twist whatsoever. This represents a difficult design challenge.

This problem is common in flying wing aircraft as well. If the washout is taken away, then the only way a flying wing can be both stable and trimmed is to reflex the trailing edge of at least a portion of the wing. There is an alternate solution in the case of the wing sail, which is to use a multi-segment flap and trim part of the flaps in one direction and part in the other. By definition, however, this means dumping lift. Therefore, this cannot be as efficient as any other viable solutions.

Free-Floating Canard

The last configuration analyzed was the free-floating canard configuration, pictured in Figure 5-23. There are also tri-surface configurations, but these were considered too complex for implementation. The free-floating canard is an unusual configuration that was first used on the 1942 Curtiss XP55 Ascender, without a great deal of success. Anecdotally, the Ascender suffered from spin recovery problems that caused its test pilots to mispronounce the aircraft's name in a pejorative sense, describing the attitude in which it flew once stalled. Note that after much work, the Ascender's problems were solved, but it remained an army project that never went into production.

What makes this configuration unique is that the canard itself is allowed to pivot freely in pitch, and is trimmed via a trailing edge flap. Thus, a change in wind direction or a gust causes the canard to rotate into a new trim position, which then, in turn, rotates the wing to its new equilibrium position. The key is that the canard itself is passively stable, and that the entire system retains stability.

There remains a quandary about stall into which this simplified analysis did not delve, but which requires some discussion. At stall, the main wing will lose lift, however the free-floating canard will not. The main wing will also gain in nose down pitching moment at stall, due to the separated flow off the back of the main wing section. The loss of lift on the main wing tends to pitch the nose upwards, increasing the stall. The increase in pitching moment

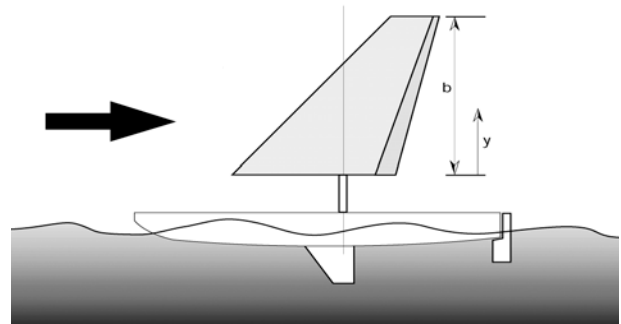


Figure 5-20 Flying wing configuration for wing sail propulsion. The flying wing has many obvious advantages. The flying wing can be made mass balanced with little or no additional ballast. Additionally, it can have the minimum swept radius of any design. The difficult is in achieving both trim and stability with no twist. Flying wings on aircraft rely on wing twist to provide both stability and trim

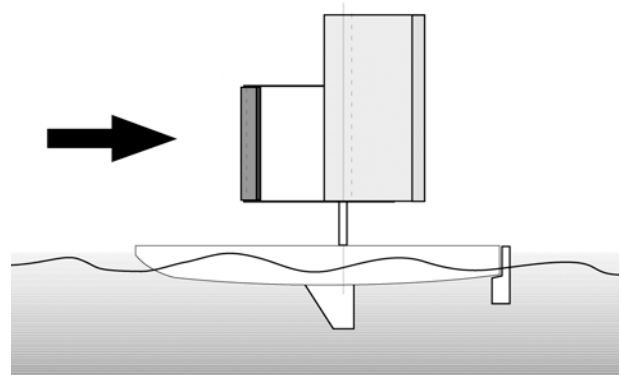


Figure 5-23 The free-floating canard configuration as it would be applied to the Atlantis. The front canard has its own trailing edge flap and is allowed to rotate about a pivot forward of the canard quarter chord line. This, in turn, drags the wing around to a new angle of attack. This system was used on the 1942 Curtiss XP55 Ascender. While it can be made passively stable, the configuration suffers large excursions during stall.

tends to pitch the nose down, decreasing the stall. The canard itself contributes nothing but its steady lift, which tends to increase the stall. Thus, at stall, the main wing must increase its pitching moment faster than the moment generated by the loss of lift and the moment arm to the center of mass. The original design of the Ascender did not achieve this balance and suffered from a divergent stall that pitched the aircraft over onto its back. Eventually, the designers realized the problem and fixed the aircraft. The only fix was in the main wing, as the canard played no role in the transient.

Results

After analyzing the four different possible configurations for trim and stability, it can be seen that only two configurations are viable: the conventional tail and the freefloating canard. The normal canard cannot be both stable and trimmed with a trailing edge flap, and the flying wing needs to reflex the trailing edge for stability, thus reducing the attainable maximum lift coefficient.

The tail volume requirement for the free-floating canard is almost double that of the conventional configuration. In addition, the free-floating canard is mechanically much more complicated, with another pivot point and an additional flap on the trimming surface. The main benefit is a much reduced swept radius, which might allow the wing to be built inside the original mast's guy wires.

Upon completing the calculations, however, the required tail volume for the free floating canard was found to be such that it, too, would require a free-standing stub-mast, without guy wires. Thus, the only advantage of the free-floating canard is effectively cancelled, and the Atlantis was fitted with a wingsail and conventional tail layout, as shown in Figure 5-16.

Conclusions

This thesis is a systems work, with contributions in structures, fluid mechanics, and guidance navigation and control areas. The main contribution detailed in this [extract from the] thesis [is]: *To describe an optimization scheme for symmetric wingsail section based on requirements unique to sailing vehicles.*

The basis for the propulsion system is a symmetric wingsail that was designed to achieve a high maximum lift coefficient with a simple flap at the Reynolds numbers appropriate to sailing vehicles. The details of this design include the requirements, development of specifications, and full analysis. The wing and tail sections are developed with a flat rooftop pressure distribution and boundary layer transition strip followed by a very gradual pressure recovery.

Using a simple trailing edge flap obviates the need for the more exotic solutions to maximum lift coefficient, such as over-the-top tacking, while preserving the ability to sail on either side of the wind. The optimization of the flap to chord ratio of the trailing edge flap results in the non-intuitive answer of a small (13%) flap with large deflection to retain the high lift to drag ratios at large coefficients of lift.

References

- [1] Amateur Yacht Research Society, *Wingsails*, AYRS Publications #14, AYRS, London, 1957.
- [8] Baker, R.M., *Tests of a Rigid-Airfoil Sails using a shore-based test stand*, The Ancient Interface IX, Proceedings of the Ninth AIAA Symposium on the Aer/Hydrodynamics of Sailing, AIAA Lecture Series, Vol. 23, AIAA Pamaona, 1979. Pages 25-60.
- [25] Birchill, J., *The Windform Sail*, The Ancient Interface II, Proceedings of the Second AIAA Symposium on the Aer/Hydrodynamics of Sailing, AIAA Lecture Series, Vol. 9, AIAA Los Angeles, 1970. Pages 59-73.
- [26] Quinton, R., Boatek website, [now at] <<http://www.boatek.club24.co.uk/>>
- [28] Bradfield, W. S., *Predicted and Measured Performance of a Daysailing Catamaran*, Marine Technology, January 1970. Pages 21-37.
- [34] Cornell University RAFT project website
- [39] Drela, M., *A new transformation and integration scheme for the compressible boundary layer equations, and solution behavior at separation*, MIT GITL Report #172, MIT Press, May 1983.
- [40] Drela, M., *XFOIL: An Analysis and Design System for Low Reynolds Number Airfoils*, Conference on Low Reynolds Number Airfoil Aerodynamics, University of Notre Dame, June 1989.
- [41] Drela, M., XFOIL website <<http://raphael.mit.edu/xfoil/>>
- [48] Fekete, G. I., Newmann, B. G., *Design and Testing of a Sailboat with Self-Trimming Wingsail*, Canadian Aeronautics and Space Journal, Vol. 29, No. 2, June 1983. Pages 121-130.

- [84] Kroo, I., PANDA website <<http://www.desktopaero.com/PANDACatalogPage.html>>
- [85] Kroo, I., McGeer, T., *Optimization of Canard Configurations*, 13th ICAS Congress, ICAS-82-6.8.1, 1982
- [92] Marchaj, C. A., *Aero-hydrodynamics of sailing*, 3rd Edition, Adlard Coles Nautical, London, 2000.
- [93] Marchaj, C. A., *Sail performance: techniques to maximize sail power*, International Marine, Camden, ME, 1996.
- [94] Marchaj, C. A., *Sailing Theory and Practice*, Dodd and Mead Co., New York, 1964.
- [98] McGeer, T., Kroo, I., *A Fundamental Comparison of Canard and Conventional Configurations*, Journal of Aircraft, Nov. 1983
- [118] Ross, J. C., *Aerodynamic Design of a Rigid-Wing Sail for a C-Class Catamaran*, The Ancient Interface XVIII, Proceedings of the Eighteenth AIAA Symposium on the Aer/Hydrodynamics of Sailing, AIAA Lecture Series, Vol. 35, AIAA Stanford, 1989.
- [122] Selig, M. S., Donovan, J. F., Fraser, D. B., *Airfoils at Low Speeds*, H.A. Stokley, Virginia Beach, VA 1989.
- [123] Shevell, R. S., *Fundamentals of Flight*, Prentice-Hall, NJ 1983, Page 170.
- [The next extract from Dr Elkaim's PhD Thesis will address the structural requirements and the construction of the wingsail. Copies of the full thesis are obtainable from Dr Elkaim, who is now Assistant Professor of Computer Engineering at the University of California at Santa Cruz; webpage: <<http://www.soe.ucsc.edu/~elkaim/>> - Editor.]